

## Genipin 가교된 키토산/산화티타늄 나노복합체의 항균성을 포함한 특성 분석

Yangshuo Liu<sup>†</sup>, Jiange Lu, Ming Li, and Chiyang He

College of Chemistry and Chemical Engineering, Wuhan Textile University  
(2015년 10월 10일 접수, 2015년 12월 13일 수정, 2015년 12월 19일 채택)

### Characterization and Antibacterial Properties of Genipin-crosslinked Chitosan/TiO<sub>2</sub> Nanocomposites

Yangshuo Liu<sup>†</sup>, Jiange Lu, Ming Li, and Chiyang He

College of Chemistry and Chemical Engineering, Wuhan Textile University, Wuhan 430074, China  
(Received October 10, 2015; Revised December 13, 2015; Accepted December 19, 2015)

**Abstract:** Novel nanocomposite films consisting of genipin-crosslinked chitosan (GC), poly(ethylene glycol) (PEG), titanium dioxide (TiO<sub>2</sub>), and silver (Ag) nanoparticles were prepared containing various amounts of TiO<sub>2</sub> and Ag nanoparticles. The effects of composition and TiO<sub>2</sub> nanoparticles on the physico-chemical properties of nanocomposite samples were evaluated by X-ray diffraction and infrared analysis. The greatest swellings were observed in the acidic pH. GC/PEG/TiO<sub>2</sub>/Ag nanocomposite showed the pH-sensitive swelling behavior and the improved mechanical properties. These nanocomposites were shown to have antibacterial activity towards *Escherichia coli*. GC/PEG/TiO<sub>2</sub>/Ag composite films had higher antimicrobial activities than GC/PEG and GC/PEG/TiO<sub>2</sub> nanocomposite films. GC/PEG/TiO<sub>2</sub>/Ag composite films have potential application as wound dressings.

**Keywords:** chitosan, swelling, titanium dioxide, silver, antimicrobial activity, wound dressing.

## Introduction

The main aim of wound healing is a speedy recovery with minimal scarring and maximal function. Dressing materials may inhibit bleeding, protect the wound from environmental irritants, absorb the wound fluids and exudates, minimize the wound surface necrosis, prevent the wound dryness, stimulate the growth rate, be elastic, non-toxic, non-antigenic, biocompatible, biodegradable dressing materials, and prevent invasion of microorganisms. Even though antibiotics have been greatly improved to deal with the increasing drug resistance of pathogens, it is also necessary to find advanced dressing materials which increase the drug resistance of pathogens effectively.<sup>1-4</sup> The selection of materials is very important from wound healing application point of views.

Titanium dioxide (TiO<sub>2</sub>) has attracted wide interest because of its good photocatalytic activity, high stability, and low price.<sup>5-8</sup> TiO<sub>2</sub> is an effective biological material used widely in

biomedical research because of its unique physiochemical nature.<sup>9</sup> Furthermore, the ability of TiO<sub>2</sub> to improve the antibacterial performance of coatings has been proven.<sup>10</sup> Titanium dioxide can create electron-hole pairs as a result of UV radiation.

Silver nanoparticles deposited in a TiO<sub>2</sub> film (Ag-TiO<sub>2</sub>) have attracted more and more attention because TiO<sub>2</sub> is a promising material as aforementioned and Ag is a nontoxic precious metal with remarkable catalytic activity<sup>11-14</sup> and size- and shape-dependent optical properties under visible light.<sup>15,16</sup> Silver ion was effectively reduced to nanophased silver on the surface of molecular-imprinted biosorbent by TiO<sub>2</sub> photocatalysis.<sup>17</sup> It is known that silver nanoparticles (Ag NPs) significantly enhance antibacterial activity.

Chitosan is a bio-compatible and biodegradable polycationic polysaccharide widely used in cosmetic and pharmaceutical industry as the drug carriers and antimicrobial activity.<sup>18,19</sup> However, chitosan is difficult to apply to pharmaceutical industry because the chitosan film is very rigid and needs the plasticization. Poly(ethylene glycol) (PEG) is one of a limited number of synthetic polymers approved by the US Food and Drug Administration. PEG is frequently used in the production

<sup>†</sup>To whom correspondence should be addressed.  
E-mail: liuyangshuo3070@163.com  
©2016 The Polymer Society of Korea. All rights reserved.

of polymer blends and could improve the flexibility and ductility of polymer by blending with the rigid polymer. Genipin, the metabolite of geniposide, is a natural product present in the fruit of *Gardenia jasminoides*. It has been used over the years in traditional Chinese medicine to treat symptoms of type 2 diabetes.<sup>20,21</sup> Hydrogels composed of PEG and chitosan possess many advantages compared to the pure chitosan films. Chitosan and PEG-based membranes were prepared using glucose-mediated process.<sup>22</sup> The use of genipin as crosslinker instead of glutaraldehyde-fixed tissue allows for genipin can form stable crosslinked products with enzymatic degradation resistance.

The crosslinking reaction mechanisms for chitosan with genipin are different at different pH values. Under acidic and neutral conditions, a nucleophilic attack by the amino groups of chitosan on the olefinic carbon atom at C-3 occurs, followed by opening the dihydropyran ring and attacked by the secondary amino group on the newly formed aldehyde group. Under basic conditions, the ring-opening reaction of genipin occurs via a nucleophilic attack by hydroxyl ions in aqueous solution to form intermediate aldehyde groups, which subsequently undergo aldol condensation. The terminal aldehyde groups on the polymerized genipin undergoes a Schiff reaction with the amino groups on chitosan to form crosslinked networks. Polyethylene are synthetic hydrophilic polymers widely used. In order to understand the effect of a crosslinker such as genipin, it was appropriate to study blends of chitosan. For example, chitosan and 80% hydrolyzed polyethylene were used to prepare semi-interpenetrating networks of varying ratios of the constituents.<sup>23</sup>

This study aims to investigate the feasibility of a novel nanocomposite of genipin-crosslinked chitosan (GC)/PEG film in which various amounts of TiO<sub>2</sub> nanoparticles were embedded for the wound-dressing applications. In this study, GC/PEG/TiO<sub>2</sub>/Ag nanocomposite films with high antibacterial activities were successfully prepared via sol-cast transformation. The antibacterial efficiency of TiO<sub>2</sub> nanoparticles in GC/PEG hydrogels was investigated in terms of the characteristics of GC/PEG/TiO<sub>2</sub>/Ag nanocomposites. The antibacterial efficiency of the nanocomposites against *Escherichia coli* was analyzed for judging the feasibility of their use as wound dressings.

## Experimental

**Materials.** TiO<sub>2</sub> and Ag nanoparticles (<100 nm, 99.5%

trace metals basis) were obtained from Aldrich Chemicals. Genipin and chitosan were purchased from Sigma. PEG (*M<sub>w</sub>* 4000) was purchased from Sigma-Aldrich. Acetic acid was purchased from Sigma. The cell culture was done in Hubei Key Laboratory of Biomass Fibers and Eco-Dyeing & Finishing, Wuhan Textile University.

**Preparation of GC/PEG/TiO<sub>2</sub>/Ag Nanocomposites.** Aqueous chitosan solution of 0.3% (w/v) was prepared by dissolving chitosan powder in aqueous 1.5% (v/v) acetic acid solution. Chitosan/PEG/TiO<sub>2</sub>/Ag solutions were prepared by mixing chitosan and PEG with various amounts of TiO<sub>2</sub> and Ag nanoparticles. The suspension was stirred overnight until complete dissolution of chitosan was achieved. Subsequently, 0.4 wt% of genipin was dissolved in 5 mL of water and then was added to the chitosan/PEG/TiO<sub>2</sub>/Ag mixed solutions under stirring for 8 h to obtain a uniformly distributed and viscous solution. Films were prepared by casting the GC/PEG/TiO<sub>2</sub>/Ag nanocomposites onto dishes. They were dried at room temperature for 24 h. All films were neutralized in a 0.1 M NaOH solution for about 10 min, washed thoroughly with distilled water, and then further vacuum dried to remove any residual solvent. GC/PEG/TiO<sub>2</sub>/Ag nanocomposite films were stored in a desiccator for further experiments. The formulation of GC/PEG/TiO<sub>2</sub>/Ag composites is shown in Table 1.

**Microorganisms.** The antibacterial activity of the prepared GC/PEG/TiO<sub>2</sub>/Ag nanocomposites were tested against four strains. *Escherichia coli* and *P. aeruginosa* are the gram-negative bacteria. *S. aureus* and *B. subtilis* are the gram-positive bacteria.

**Characterization of GC/PEG/TiO<sub>2</sub>/Ag Nanocomposites.** Fourier transform infrared attenuated total reflectance (FTIR-ATR) spectra of chitosan, PEG, GC/PEG interpenetrating polymer network, and GC/PEG/TiO<sub>2</sub>/Ag nanocomposite films were recorded at room temperature by FTIR spectroscopy

**Table 1. Feed Compositions of GC/PEG/TiO<sub>2</sub>/Ag Films**

Sample name	Chitosan (g)	PEG (g)	TiO <sub>2</sub> (g)	Ag (mg)
GC/PEG-1	0.4	0.1	0	0
GC/PEG-2	0.4	0.1	0.01	0
GC/PEG-3	0.4	0.1	0.02	0
GC/PEG-4	0.4	0.1	0.04	0
GC/PEG-5	0.4	0.1	0.01	1
GC/PEG-6	0.4	0.1	0.02	1
GC/PEG-7	0.4	0.1	0.04	1
GC/PEG-8	0.4	0.1	0	1

(FTS 175C, U.S.A.) in the range 4000-600 cm<sup>-1</sup>. X-ray diffraction analyses were obtained with a RINT2000 X-ray diffractometer. The scanning of diffraction angle 2θ was between 5° and 70°. The mechanical properties were measured by Instron type universal testing machine (Instron 4200, U.S.A.) at room temperature, with a tensile speed of 10 mm/min.

**Swelling Study.** The swelling behavior of GC/PEG/TiO<sub>2</sub>/Ag films was immersed in the buffers of various pHs at room temperature. The swollen hydrogel films were removed at pre-determined intervals and weighed immediately after blotting with a filter paper to remove the surface water, followed by immediate weighing. The swelling ratio was calculated with the following equation:

$$\text{Swelling ratio (\%)} = (W_t - W_0) / W_0 \times 100$$

where  $W_t$  and  $W_0$  are the weights of the samples in the swollen and dry states, respectively. The swelling ratios were measured for five samples of each hydrogel, and the average of the five values was plotted against the pH value.

**Evaluation of Antimicrobial Activities.** *In-vitro* antimicrobial activities of GC/PEG/TiO<sub>2</sub>/Ag nanocomposite films were evaluated by adopting the zone inhibition method. Herein, two bacteria strains including the gram-positive *S. aureus* and the gram-negative *E. coli* were examined. The bacteria were cultured in a nutrient agar at 37 °C for 24 h. GC/PEG/TiO<sub>2</sub>/Ag nanocomposite films of 2 mm diameter were then added and the mixtures of GC/PEG/TiO<sub>2</sub>/Ag nanocomposite and *E. coli* were placed at 37 °C in a shaking incubator for 6 h.

The disks were then placed on the surface of a sterilized agar nutrient medium that was inoculated with the test bacteria. Then, the inoculated plates were incubated at 37±1 °C for 24 h. The agar plate is divided into 4 sections GC/PEG, GC/PEG/TiO<sub>2</sub>, GC/PEG/Ag, and GC/PEG/TiO<sub>2</sub>/Ag sample. Then the zone of inhibition of growth was measured, which indicates the inhibitory activity of each compound on the growth of the bacteria.

## Results and Discussion

**FTIR Spectroscopy.** Figure 1 shows the FTIR-ATR spectra of GC, GC/PEG, GC/PEG/TiO<sub>2</sub>, and GC/PEG/TiO<sub>2</sub>/Ag films. GC/PEG film has shown absorption peaks at 1662, 1596, and 1338 cm<sup>-1</sup> relating to amide I, amide II of C=O stretching vibrations, and N-H bending vibrations, respectively. The curved shows that the peaks at 3412 and 1078 cm<sup>-1</sup> that, a ref-

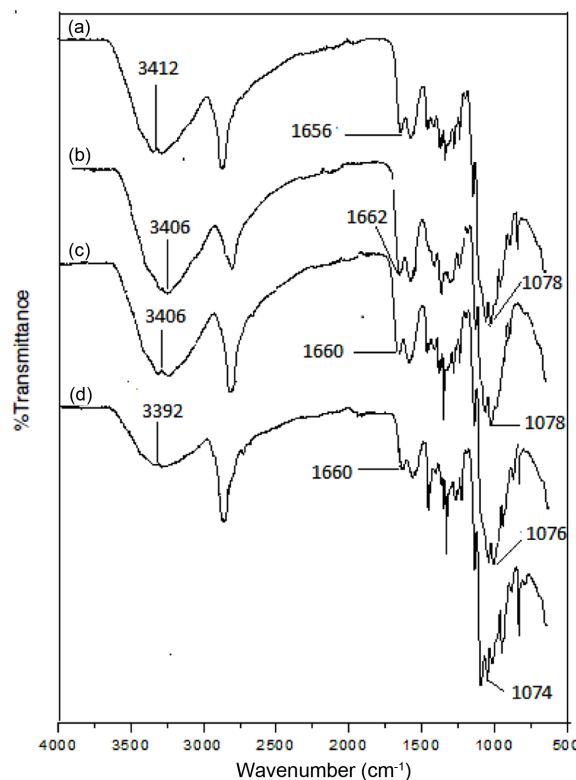


**Figure 1.** FTIR spectra of (a) GC; (b) GC/PEG; (c) GC/PEG/TiO<sub>2</sub>; (d) GC/PEG/TiO<sub>2</sub>/Ag films.

erence to the N-H and O-H groups, were shifted to 3392 and 1074 cm<sup>-1</sup> became broader and stronger for GC/PEG/TiO<sub>2</sub>/Ag nanocomposite film.<sup>24,25</sup> The FTIR spectra of composite GC/PEG/TiO<sub>2</sub> shows more peaks than that of GC and GC/PEG, but TiO<sub>2</sub> in the film has no obvious effect on the peak of N-H and OH. The reason for the above phenomena was that the polarity of the hydrogen bonds between chitosan was enhanced when silver ions combined with chitosan.

**Surface Morphology.** Figure 2 presents the SEM micrographs of the surfaces of GC/PEG and GC/PEG/Ag nanocomposite. The GC/PEG (Figure 2(a)) showed the smooth surface morphology. Silver nanoparticles were uniformly distributed on the surface of GC/PEG/Ag nanocomposite without severe aggregation (Figure 2(b)). The GC/PEG/Ag/TiO<sub>2</sub> nanocomposite film has smooth surface texture and the spherical silver and TiO<sub>2</sub> nanoparticles with diameters of about 15-20 nm and 40-60 nm were observed, respectively. Silver and TiO<sub>2</sub> nanoparticles were distributed uniformly in the GC/PEG/Ag/TiO<sub>2</sub> nanocomposite.

**X-ray Diffraction.** Figure 3 shows the XRD patterns of GC/PEG, GC/PEG/TiO<sub>2</sub>, and GC/PEG/TiO<sub>2</sub>/Ag nanocomposite

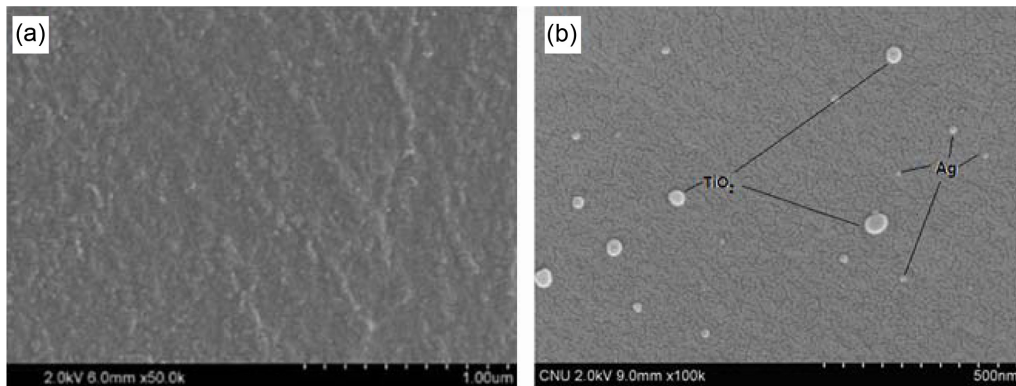


**Figure 2.** SEM images of (a) GC/PEG; (b) GC/PEG/Ag/TiO<sub>2</sub> nanocomposites.

films. Two crystal forms existed in GC/PEG film (Figure 3(a)) depicting the major crystalline peaks at 10.0° and 19.8°, respectively. These two main XRD peaks of GC/PEG shifted to 10.1° and 20.2° for GC/PEG/TiO<sub>2</sub>/Ag nanocomposite film (Figure 3(c)). GC/PEG/TiO<sub>2</sub>/Ag nanocomposite film showed two additional peaks at 2θ of 26.2°, 38.0°, 48.1°, and 55.2° which were related to the TiO<sub>2</sub> crystallite<sup>26</sup> and another peak at 2θ of 38.2° and 64.5° which were characteristic of the Ag nanoparticles.<sup>27</sup> These findings indicate the possible interactions between free hydroxyl groups of chitosan and TiO<sub>2</sub> and Ag nanoparticles in the nanocomposites.

#### Swelling Behavior of GC/PEG/TiO<sub>2</sub>/Ag Nanocomposites.

The swelling behavior of GC/PEG, GC/PEG/TiO<sub>2</sub>, and GC/

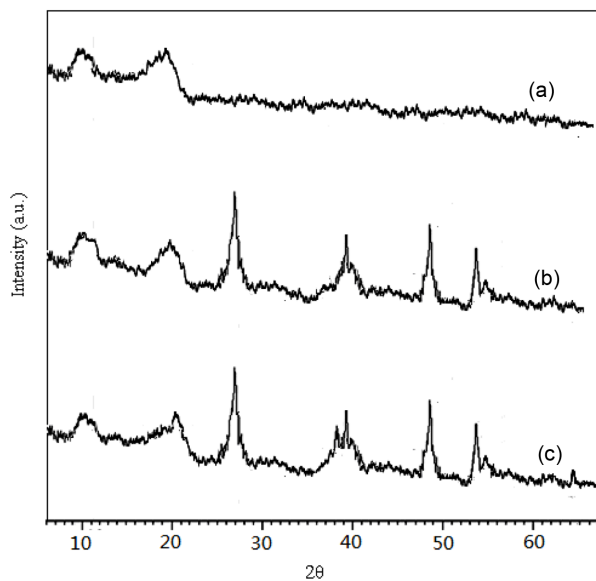


**Figure 3.** X-ray diffraction patterns of (a) GC/PEG; (b) GC/PEG/TiO<sub>2</sub> (GC/PEG-3); (c) GC/PEG/TiO<sub>2</sub>/Ag (GC/PEG-6) nanocomposite films.

PEG/TiO<sub>2</sub>/Ag nanocomposites at various pHs is shown in Figure 4. The swelling of GC/PEG matrix was pH-dependent. GC/PEG/TiO<sub>2</sub>/Ag nanocomposite swelled greatly in the acidic medium compared to the neutral or basic one. As TiO<sub>2</sub> and Ag nanoparticles were incorporated in GC/PEG matrix, the swelling decreased to some extent.

GC/PEG/TiO<sub>2</sub>/Ag nanocomposites swelled higher at a much faster rate in the acidic pH medium than in a neutral and alkaline medium. Because the amino groups reformed in the network could be protonated in a lower pH medium, the equilibrium swelling ratio of chitosan-containing hydrogel in the acidic solution was larger than that in a higher pH. In the acidic pH the NH<sub>2</sub> groups become positively charged NH<sub>3</sub><sup>+</sup> cations and thereby increase the interactions of the films with the aqueous medium.

The chitosan chain could lead to an expansion of the network and hence a higher swelling.<sup>28,29</sup>

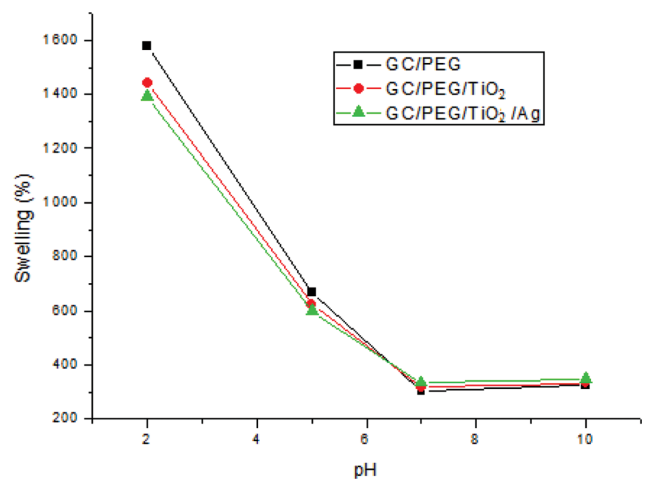


**Figure 4.** Swelling ratios of GC/PEG, GC/PEG/TiO<sub>2</sub> (GC/PEG-3), and GC/PEG/TiO<sub>2</sub>/Ag (GC/PEG-6) nanocomposites at various pHs.

Hydrogel dressings are indicated for chronic wounds which exhibit only slight exudation. Because of the high water content of up to 90% of these dressings, they are able to keep granulation tissue and fresh epithelial tissue moist and protect them from external mechanical stress and provide a barrier to secondary infection from the environment.<sup>30</sup> Various hydrogel films were used in treating the chronic wounds such as burns and ulcers because good hydration was recognized to be important for quick healing and reepithelialization of the wound.<sup>31-34</sup> However, this high swelling property of GC/PEG/TiO<sub>2</sub>/Ag dressing material is due to hydrophilic nature of material and important for quick absorption of exudates for wound healing materials.

**Mechanical Properties.** It is well known that the chitosan is developed to treat the burn wounds as antibacterial materials. However, it has limited applicability due to poor mechanical properties as well as lower rates of water absorption. The mechanical properties of GC/PEG, GC/PEG/TiO<sub>2</sub>, and GC/PEG/TiO<sub>2</sub>/Ag nanocomposite films are presented in Table 2.

**Table 2. Mechanical Properties of GC/PEG, GC/PEG/TiO<sub>2</sub>, and GC/PEG/TiO<sub>2</sub>/Ag Nanocomposite Films**

Sample name	TiO <sub>2</sub> (g)	Tensile strength (MPa)	Elongation at break (%)
GC/PEG-1	0	55.2	16.4
GC/PEG-2	0.01	68.2	21.4
GC/PEG-3	0.02	70.4	22.6
GC/PEG-4	0.04	78.2	23.3
GC/PEG-5	0.01	75.5	24.5
GC/PEG-6	0.02	76.4	26.8
GC/PEG-7	0.04	80.1	27.7
GC/PEG-8	0	59.9	17.1

Both GC/PEG/TiO<sub>2</sub> and GC/PEG/TiO<sub>2</sub>/Ag nanocomposite films generally showed the higher tensile strength compared to GC/PEG film.<sup>35</sup>

Among the various nanocomposite films, the nanocomposite films containing 2 wt% TiO<sub>2</sub> showed the highest mechanical properties. However, further increase in the TiO<sub>2</sub> content resulted in the fast deterioration of both tensile strength and elongation at break. Thus, the mechanical properties of GC/PEG film can be improved by incorporating a proper amount of TiO<sub>2</sub> because of the favorable interactions between GC/PEG and TiO<sub>2</sub> nanoparticles. When TiO<sub>2</sub> was introduced in GC/PEG matrix, this effect can be explained from the fact that the blending of PEG with chitosan leads to an intermolecular interaction forming ethereal groups between them and new hydrogen bonds were formed between GC and TiO<sub>2</sub>, which made the movement of macromolecular chain easier. This effect can be explained from the fact that the blending of PEG with chitosan leads to an intermolecular interaction forming ethereal groups between them, within a reasonable range of composition.

**Antibacterial Activity of GC/PEG/TiO<sub>2</sub>/Ag Nanocomposites.** TiO<sub>2</sub> nanoparticles embedded in GC/PEG matrix were responsible for the antibacterial activities. The antibacterial activities of GC/PEG, GC/PEG/TiO<sub>2</sub>, and GC/PEG/TiO<sub>2</sub>/Ag nanocomposite films were tested toward antibacterial activity by the inhibition zone method and presented in Table 3 and Figure 5. It was found that GC/PEG without TiO<sub>2</sub> was able to inhibit the bacterial growth to some degree. However, the inhibition zone increased significantly when the content of TiO<sub>2</sub> increased. In addition, the antibacterial activity was improved more effectively by doping TiO<sub>2</sub> with small amount of Ag. The synergistic antibacterial activity of nanocomposites could be obtained by combining TiO<sub>2</sub> and Ag nanoparticles. The inhi-

**Table 3. Diameters (mm) of the Inhibition Zone Against Bacteria**

Sample name	Gram-positive			Gram-negative	
	TiO <sub>2</sub> (g)	<i>S. aureus</i>	<i>B. subtilis</i>	<i>E. coli</i>	<i>P. aeruginosa</i>
GC/PEG-1	.0	10.1	9.2	8.0	10.5
GC/PEG-2	0.01	12.9	11.2	10.4	12.8
GC/PEG-3	0.02	13.7	13.5	12.4	13.5
GC/PEG-4	0.04	17.7	16.7	16.3	16.5
GC/PEG-5	0.01	16.4	17.0	14.7	17.1
GC/PEG-6	0.02	20.1	19.1	18.5	19.6
GC/PEG-7	0.04	25.0	24.9	24.4	23.7
GC/PEG-8	.0	11.8	12.3	9.8	11.6

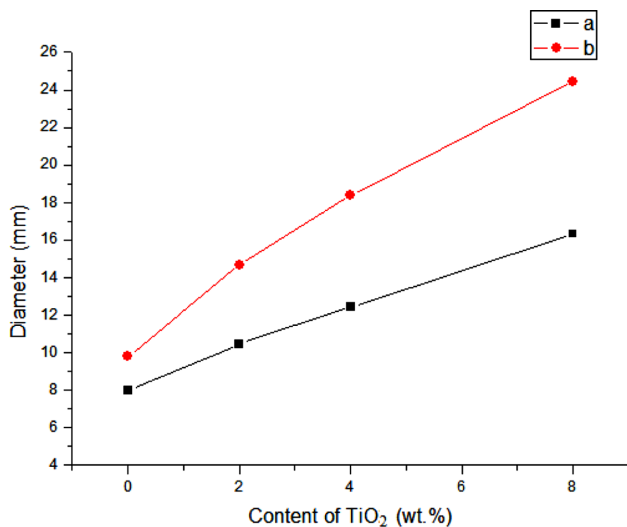


**Figure 5.** Diameters of the inhibition zone against bacteria colonies on (a) GC/PEG/TiO<sub>2</sub>; (b) GC/PEG/TiO<sub>2</sub>/Ag composite films with different mass ratios of TiO<sub>2</sub>.

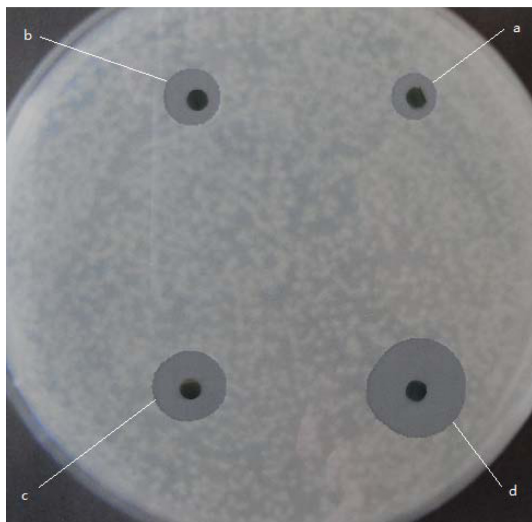


**Figure 6.** Comparison of *E. coli* inhibition zones formed by (a) GC/PEG; (b) GC/PEG/Ag; (c) GC/PEG/TiO<sub>2</sub> (GC/PEG-3); (d) GC/PEG/TiO<sub>2</sub>/Ag (GC/PEG-6) nanocomposite films.

inhibition zone against *E. coli* formed on the culture plates are displayed in Figure 6. The smallest inhibition zone of 8.0 mm was obtained for GC/PEG film (Figure 6(a)). However, the nanocomposite showed significantly improved inhibition effect on *E. coli* resulting in the inhibition zone of 12.4 mm for GC/PEG/TiO<sub>2</sub> (Figure 6(c)) and 18.5 mm for GC/PEG/TiO<sub>2</sub>/Ag (Figure 6(d)), respectively. GC/PEG films containing TiO<sub>2</sub> and Ag showed the highly improved antibacterial activity toward *E. coli*. GC/PEG/TiO<sub>2</sub>/Ag nanocomposite films pre-

pared in this work may be used as hydrophilic wound and burn dressings.

**Antimicrobial Mechanism.** Cho *et al.*<sup>36</sup> investigated the antibacterial effects of Ag NPs. They supposed that these NPs have the ability to strongly bind to sulfur- and phosphor-containing compounds and cause damage to the bacterial cell membrane by impairing sulfur-containing proteins. They can also penetrate the bacteria and damage sulfur-containing enzymes and phosphor-containing DNA. In addition, Ag NPs are also known to accumulate heavily within mitochondria and are reported to impair mitochondrial function via oxidative stress, thus ceasing the adenosine triphosphate (ATP) synthesis. Another antimicrobial mechanism is the releasing of silver ions which contribute to cell death by producing high amounts of reactive oxygen species (ROS). The extremely high surface area of nanoscaled TiO<sub>2</sub> facilitated the adsorption of target bacteria, which accelerated the rate of antibacterial reaction.<sup>37</sup> Therefore, the presence of Ag and TiO<sub>2</sub> enhanced the antimicrobial ability of chitosan significantly.

## Conclusions

GC/PEG/TiO<sub>2</sub> nanocomposites maintained the higher swelling ratios as the pH decreased to acidic condition. The presence of TiO<sub>2</sub> in GC/PEG matrix inhibited the proliferation of bacteria effectively. The antimicrobial activity of GC/PEG/TiO<sub>2</sub> nanocomposites increased as the content of TiO<sub>2</sub> increased. The TiO<sub>2</sub> with small amount of Ag nanoparticles enhancing the antimicrobial activity of nanocomposites.

GC/PEG/TiO<sub>2</sub>/Ag nanocomposites could be applied successfully as the antibacterial applications such as wound-dressing films based on both swelling and antibacterial characteristics.

**Acknowledgments:** This work was financially supported by the National Natural Science Foundation of China (51203125), and Key Project of Chinese Ministry of Education (210140).

## References

1. A. L. Harkins, S. Duri, L. C. Kloth, and C. D. Tran, *J. Biomed. Mater. Res. B*, **102**, 1199 (2014).
2. R. Deepachitra, V. Ramnath, and T. P. Sastry, *RSC. Adv.*, **4**, 62717 (2014).
3. D. Archana, B. K. Singh, J. Dutta, and P. K. Dutta, *Carbohydr. Polym.*, **95**, 530 (2013).

4. P. I. Morgado, P. F. Lisboa, M. P. Ribeiro, S. P. Miguel, P. C. Simões, I. J. Correia, and A. Aguiar-Ricardo, *J. Membrane Sci.*, **469**, 262 (2014).
5. A. Fujishima and K. Honda, *Nature*, **238**, 37 (1972).
6. I. Robel, V. Subramanian, M. Kuno, and P. V. Kamat, *J. Am. Chem. Soc.*, **128**, 2385 (2006).
7. Y. S. Ko, Y. H. Han, and J. H. Yim, *Polym. Korea*, **38**, 525 (2014).
8. S. Zheng, Y. Cai, and K. E. O'Shea, *J. Photoch. Photobio.*, **210**, 61 (2010).
9. D. Hua, K. Cheuk, Z. Wei-ning, W. Chen, and X. Chang-fa, *Trans. Nonferrous Met. Soc. China*, **17**, s700 (2007).
10. L. Caballero, K. A. Whitehead, N. S. Allen, and J. Verran, *Dyes Pigm.*, **86**, 56 (2010).
11. D. Guin, S. V. Manorama, J. N. L. Latha, and S. Singh, *J. Phys. Chem. C*, **111**, 13393 (2007).
12. I. M. Arabatzis, T. Stergiopoulos, M. C. Bernard, D. Labou, S. G. Neophytides, and P. Falaras, *Appl. Catal. B*, **42**, 187 (2003).
13. E. Z. Chen, H. J. Su, and T. W. Tan, *J. Chem. Technol. Biot.*, **86**, 421 (2011).
14. Y. C. Yang, J. W. Wen, J. H. Wei, R. Xiong, J. Shi, and C. X. Pan, *Appl. Mater. Inter.*, **5**, 6201 (2013).
15. Y. Ohko, T. Tatsuma, T. Fujii, K. Naoi, C. Niwa, Y. Kubota, and A. Fujishima, *Nat. Mater.*, **2**, 29 (2003).
16. K. Naoi, Y. Ohko, and T. Tatsuma, *J. Am. Chem. Soc.*, **126**, 3664 (2004).
17. H. Y. Huo, H. J. Su, W. Jiang, and T. W. Tan, *Biochem. Eng. J.*, **43**, 2 (2009).
18. X. Xi, W. J. Zhen, S. Z. Bian, and W. T. Wang, *Polym. Korea*, **39**, 601 (2015).
19. R. A. A. Muzzarelli, R. Tarsi, O. Filippini, E. Giovanetti, G. Biagini, and P. E. Varaldo, *Antimicrob. Agents Ch.*, **34**, 2019 (1990).
20. Y. Danbuo, *The Essential Methods for Miscellaneous Diseases*, 2nd Edn, Y. Wang, Editor, People's Health Publishers, PR China, 1984.
21. S. Shindo, Y. Hosokawa, I. Hosokawa, K. Ozaki, and T. Matsuo, *Biochimie*, **107**, 391 (2014).
22. J. W. Wang and M. H. Hon, *J. Appl. Polym. Sci.*, **96**, 1083 (2005).
23. R. A. A. Muzzarelli, *Carbohydr. Polym.*, **77**, 1 (2009).
24. D. W. Wei, W. Y. Sun, W. P. Qian, Y. Z. Ye, and X. Y. Ma, *Carbohydr. Res.*, **344**, 2375 (2009).
25. E. Günister, D. Pestreli, C. H. Ünlü, O. Atıcı, and N. Güngör, *Carbohydr. Polym.*, **67**, 358 (2007).
26. Y. Kitkulnumchai, A. Ajavakom, and M. Sukwattanasinitt, *Cellulose*, **15**, 599 (2008).
27. S. A. Amin, M. Pazouki, and A. Hosseinnia, *Powder Technol.*, **196**, 241 (2009).
28. A. S. Carreira, F. A. M. M. Gonçalves, P. V. Mendonça, M. H. Gil, and J. F. J. Coelho, *Carbohydr. Polym.*, **80**, 618 (2010).
29. Z. Shariatinia and M. Fazli, *Food Hydrocoll.*, **46**, 112 (2015).
30. S. Seaman, *J. Am. Podiat. Med. Assn.*, **92**, 24 (2002).
31. M. A. Amin and I. T. Abdel-Raheem, *Arch. Pharm. Res.*, **37**, 1016 (2014).
32. S. P. Tan, P. McLoughlin, L. O'Sullivan, M. L. Prieto, G. E. Gardiner, P. G. Lawlor, and H. Hughes, *Int. J. Pharm.*, **456**, 10 (2013).
33. R. Pereira, A. Carvalho, D. C. Vaz, M. H. Gil, A. Mendes, and P. Bartolo, *Int. J. Biol. Macromol.*, **52**, 221 (2013).
34. J. Moore and A. Perkins, *Adv. Skin Wound Care*, **23**, 544 (2010).
35. K. A. M. Amin and M. Panhuis, *Polymers*, **4**, 590 (2012).
36. K. H. Cho, J. E. Park, T. Osaka, and S. G. Park, *Electrochim. Acta*, **51**, 956 (2005).
37. M. Kanna and S. Wongnawa, *Mater. Chem. Phys.*, **110**, 166 (2008).